PERGAMON

International Journal of Heat and Mass Transfer 41 (1998) 4315–4325

International Journal of HEAT and MASS TRANSFER

Mass transfer of CO_2 through liquid CO_2–water interface

Ho Teng[a,*], Akihiro Yamasaki[b]

[a] *Department of Mechanical Engineering, The Hong Kong University of Science and Technology, Clear Water Bay, Kowloon, Hong Kong*

[b] *National Institute of Materials and Chemical Research, 1-1 Higashi, Tsukuba, 305, Japan*

Received 11 April 1997; in final form 6 February 1998

Abstract

An experimental investigation on mass transfer of CO_2 through the liquid CO_2–water interface is reported. At high pressures and low temperatures, water at the liquid CO_2–water interface has a quasi-crystalline structure which, locally, may resemble a hydrate crystal element. If the pressure and temperature of the system fall within the hydrate-formation region, then hydrate will form rapidly at the interface; in this case, the quasi-crystal becomes a true crystal. It is found in this study that the interfacial crystallization does not cause a dramatic decrease in the rate of mass transfer, and for both cases with and without an interfacial hydrate layer the overall mass-transfer coefficients are of order of 10^{-7} m s^{-1}. A mechanism for the interfacial mass-transfer is proposed, which reasonably explains the behavior of the interfacial hydrate layer.

Nomenclature

C concentration of CO_2 in water
C_0 density of CO_2 [kmol m^{-3}]
C_{app} apparent CO_2 concentration
C_h concentration of hydrate clusters
C_H density of CO_2 hydrate [kmol m^{-3}]
D diffusion coefficient of CO_2 in water
D_H interstitial diffusion coefficient of CO_2 in hydrate
f_{CO_2} fugacity of CO_2
$f^0_{CO_2}$ fugacity of pure liquid CO_2
H dimensionless concentration of hydrate clusters
K overall mass-transfer coefficient
K_d overall mass-transfer coefficient for CO_2 droplet
K_f mass-transfer coefficient based on fugacity
l length of liquid CO_2 column
$\dot{m}$ rate of mass transfer
M_{CO_2} molar mass of CO_2
n hydrate number
p pressure
r radius of CO_2 droplet
t time
T temperature
t_f hydrate formation time
x distance from interface
y_{CO_2} mole fraction of CO_2.

Greek letters
γ_{CO_2} activity coefficient of CO_2
δ hydrate layer thickness
κ reaction rate constant
ρ_{CO_2} density of liquid CO_2 [kg m^{-3}].

Subscripts
cr property at minimum hydrate stability
s property at interface
w property of bulk water.

Superscripts
H hydrate phase
W bulk water phase.

1. Introduction

Disposal and sequestration of anthropogenic CO_2 in deep waters (depths > 3000 m) in the ocean has been proposed by many investigators as a means to mitigate global warming [1–4]. Under conditions of deep-ocean waters, CO_2 is in liquid state and denser than sea water.

* Corresponding author. Fax: 852-2358-1543; e-mail: mehoteng@uxmail.ust.hk

0017–9310/98 $19.00
PII: S0017–9310(98)000173–2

It is believed that if the disposal process is controlled properly, then the liquid CO_2 disposed of in the deep ocean would form a lake on the sea floor [5–13]. Owing to hydrodynamic instability, the liquid CO_2 effluent may break up into droplets and these droplets may be covered with a thin hydrate layer [5–10]. This suggests that the CO_2 lake be formed with discrete liquid elements (droplets) which are separated by a hydrate interphase, i.e., the CO_2 lake may not be a continuous fluid phase. However, the inside structure of the CO_2 lake may not influence mass transfer between the CO_2 and sea water which occurs only at the surface of the CO_2 lake.

Dissolution of a CO_2 droplet in high-pressure and low-temperature water was investigated previously [5–9, 13]. It was found in the previous investigations that if a CO_2 droplet was released in water at $T \leqslant 10^{\circ}C$ and $p \geqslant 45$ bar, then a thin hydrate layer would form rapidly on the surface of the droplet. The interfacial hydrate layer was found not to stop mass transfer as long as the water was unsaturated with CO_2. Almost all of the previous investigations on dissolution of liquid CO_2 in water focused on the shrinkage of a CO_2 droplet and the phenomenon of the interfacial mass transfer was not studied in detail. To date, no investigation on mass transfer at a planar liquid CO_2–water interface has been reported. Thus, behavior of the surface of the CO_2 lake (a liquid CO_2–sea water interface) and mechanism for the interfacial mass transfer are not well understood. To fill that void, this study examines behavior of and mass transfer at the liquid CO_2–water interface.

2. Phenomena of mass transfer at liquid CO_2–water interface

2.1. Characteristics of the liquid CO_2–water system

Since mass transfer in the liquid CO_2–water system differs from that in many other liquid–liquid systems often encountered in the engineering applications, the characteristics of the liquid CO_2–water system are briefed in the following.

In a binary liquid–liquid system, generally, the two pure components are mutually soluble; thus the terms solute and solvent become somewhat arbitrary. However, if the system is only slightly soluble and highly asymmetric, then it may be treated as a one-sided solubility system [14]. CO_2 and water are highly thermodynamically dissimilar [15]. Under conditions in the deep ocean, the solubility of liquid CO_2 in water ($\sim$4.0 mol%) is larger than that of water in liquid CO_2 (< 0.1 mol%) by one order of magnitude. Therefore, it is reasonable to treat the liquid CO_2–water system as a one-sided solubility system, with liquid CO_2 as the solute and water as the solvent. This one-sided solubility feature greatly simplifies modeling of the interfacial mass transfer because it implies that mass transfer at the liquid CO_2–water interface occurs in one way: only CO_2 diffuses through the interface. Since molecular diffusion in liquids, as in solids, has a kinetic mechanism [16] which is influenced by the local structure, the structure of the interfacial water plays an important role in controlling the rate of mass transfer.

Structure of water at the liquid CO_2–water interface depends largely on the characteristics of water. The water molecule has four charges: the two positive charges are given by the shared electrons with the protons and the two negative charges are formed by the lone pairs of electrons. Each water molecule therefore can be attached to four other water molecules through four hydrogen bonds by donating two and receiving two. Owing to molecular interactions and hydrogen bonding of water molecules, liquid water has a very complicated local structure (note that a liquid is ordered only locally). Large amounts of water molecules in liquid water exist in the form of hydrogen-bonded ring structure, i.e., five- and six-membered polygons. Hydrogen bonds in these pentagonal and hexagonal rings are arranged in such a way that they tend to share edges to form polyhedral cavities. Because water molecules are bonded with geometrical distortions in these cavities, such cavities are unstable under their own attractive forces and electrostatic interactions with water molecules in the neighborhood. Although diameters of water cavities are less than 10 Å, these cavities are large enough to allow some small, nonpolar solute molecules to enter if their sizes are smaller than the free diameters of the cavities. The presence of a solute molecule (as the guest) in a water cavity (as the host) modifies the distorted hydrogen bonding through the host–guest interactions and hence stabilizes the cavity. If the stabilized cavities are associated with each other, then a tridymite-like crystalline structure, i.e., hydrate, may be formed; however, hydrate is thermodynamically stable only at high pressures and low temperatures. Because the solute mole fraction in hydrate is much larger than solubility of the solute in water, hydrate formation requires that the system be highly supersaturated; therefore, without agitation, the solute–water interface is the only location for hydrate to form, i.e., hydrate formation occurs only as an interfacial phenomenon. Many liquids encountered in engineering applications are either polar substances or with too large molecular sizes; thus the aforementioned phenomenon does not occur in systems formed by such solutes and water.

CO_2 is a nonpolar substance and its molecular diameter (5.12 Å) is smaller than the free diameter (5.76 Å) of most of water cavities; thus CO_2 molecules may enter water cavities (here only cavities related to CO_2 are of interest). Although the CO_2 concentration may be negligible in the bulk water (as in the ocean), at the liquid CO_2–water interface water can be highly supersaturated

with CO_2. Owing to reorientation of water molecules induced by the polar (water)–nonpolar (CO_2) interactions and supersaturation with CO_2, the interfacial water becomes more highly ordered than the bulk water, implying that more polyhedral cavities form in the interfacial water. If the system pressure is greater than 45 bar and the system temperature is less than 10°C, then hydrate will form at the interface. (Note that conditions for hydrate formation from gaseous CO_2 are different from those discussed here; however, these conditions cannot be satisfied in the ocean, i.e., hydrate cannot be formed from gaseous CO_2 in the ocean.) The unit crystal cell of CO_2 hydrate has a pseudo body-centered structure formed by a linkage of 46 water molecules with two pentagonal-dodecahedral cavities and six tetrakaidecahedral cavities. If all the cavities are occupied by CO_2 molecules (note that each cavity can hold at most one CO_2 molecule), then the chemical formula for CO_2 hydrate is $8CO_2 \cdot 46H_2O$ or $CO_2 \cdot 5.75H_2O$. In reality, it is difficult for all of the cavities to be occupied; thus, CO_2 hydrate always contains fewer than the stoichiometric number of CO_2 molecules and, in practice, the chemical formula for CO_2 hydrate should be $CO_2 \cdot nH_2O$, where $n > 5.75$. Crystallization at the interface causes changes in structure of the interfacial water and hence affects the rate of the interfacial mass transfer.

2.2. Experimental system

Mass transfer through the liquid CO_2–water interface was investigated experimentally. A schematic diagram of the experimental system is shown in Fig. 1. The system consisted of a sapphire tube of 6 mm inside diameter, 260 mm in length, and 2 mm in wall thickness; a 90-mm i.d. acryl cylinder (water jacket) through which the water in a thermal bath was circulated; a water reservoir which volume was about 25 times that of the sapphire tube; a piston pump; and a pressure control unit. The temperature of the system was controlled by the thermal bath with an accuracy of ± 0.2°C. The pressure of the system was controlled by the piston pump and the pressure control unit. The high-pressure side (pressurizing chamber) of the pump which was filled with water and connected with the water reservoir, and the low-pressure side (control chamber) of the pump was filled with nitrogen gas whose pressure was controlled by the pressure control unit. The pressure control unit consisted of a pressure transducer, two on/off magnetic valves which controlled the nitrogen pressure in the pressure control chamber, two needle valves which controlled the venting/filling rates of the magnetic valves, and a PID controller which controlled the actions of the magnetic valves according to the pressure difference between the set value and the value detected by the pressure transducer at the water reservoir. The system pressure could be controlled at an accuracy of ± 0.1 bar. The system was tested at 350 bar by filling with water; no leakage was found over a period of one week.

In the experiments, the water reservoir and the sapphire tube was filled with the deionized water, then CO_2 gas (with a purity > 99.99%) at room temperature was introduced from a high pressure CO_2 cylinder into the system. At the required pressure and temperature ($p > 60$ bar and $T < 20$°C) CO_2 was in liquid state, so CO_2 became liquid when it entered the system. When the desired amount of liquid CO_2 was added, the filling valve was shut off. The liquid CO_2 column (in the upper section) in the tube was then in contact with a water column (in the lower section) which connected with the water reservoir. The tests covered a range of $p = 60 \sim 300$ bar and $T = 5 \sim 18$°C. During each test, the temperature and pressure of the system were maintained at set values. The temperature was measured by a thermocouple in the water jacket, and the pressure was determined by a pressure gauge installed at the water reservoir. Changes in volume of the liquid CO_2 column due to mass transfer were determined with a scale attached to the sapphire tube in the water jacket. The behavior of the liquid CO_2–water interface could be viewed by a video camera and a monitor. In order to keep the water in the system to be highly unsaturated with CO_2, each test lasted only 5 h and then the substances tested were replaced with fresh water and liquid CO_2 for another test. Although at high pressures and low temperatures the density of liquid CO_2 may become slightly larger than that of water, owing probably to crystallization (if $T \leqslant 10$°C) or quasi-crystallization (if $T > 10$°C) at the interface and the small tube diameter as well as the wall effect on the interfacial layer, no inversion was observed, i.e., the liquid CO_2 column was remained in the upper section of the sapphire tube in all of the tests that we conducted.

2.3. Interfacial phenomena

2.3.1. Crystallization and quasi-crystallization at the interface

It has been reported by many investigators that CO_2 hydrate will form at the liquid CO_2–water interface if the system pressure and temperature fall within the hydrate-formation region, i.e., $p \geqslant 45$ bar and $T \leqslant 10$°C. Since in each test liquid CO_2 was filled at about 60 bar and then the system pressure was increased to a desired value, after filling the CO_2 and before pressurizing the interface was usually in a concave shape because the system pressure was set to be a little lower than 60 bar when filling the CO_2. It was observed that at $T < 10$°C (note that in all the tests that we conducted pressures were greater than 45 bar) when liquid CO_2 was in contact with water a thin hydrate layer formed rapidly at the interface. Although hydrate seemed to form at the interface in a few seconds, the curvature of the interface began to respond only after about $10 \sim 15$ s, indicating that it took a short period of

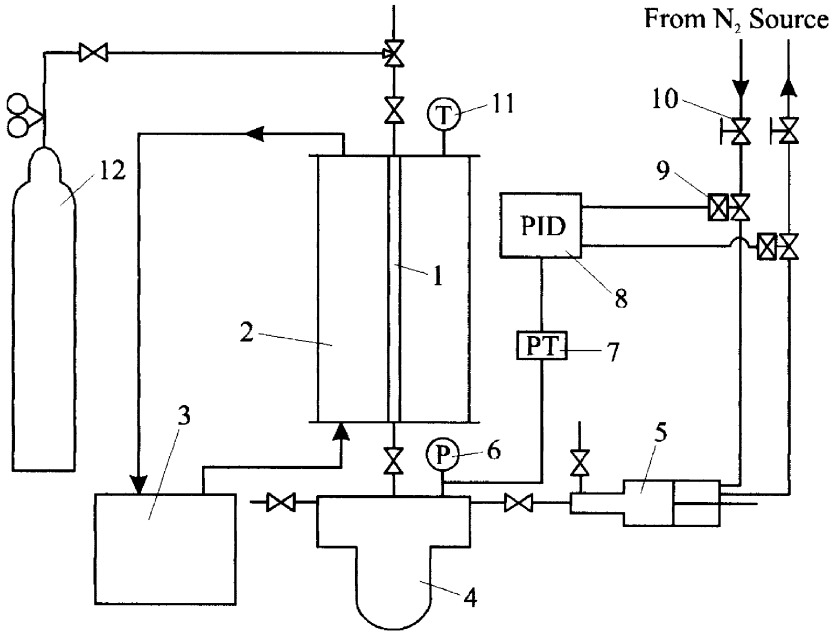

Fig. 1. Schematic diagram of experimental system. 1, Sapphire tube; 2, water jacket; 3, thermal bath; 4, water reservoir; 5, piston pump; 6, pressure gauge; 7, pressure transducer; 8, PID controller; 9, magnetic valve; 10, needle valve; 11, thermocouple; 12, CO_2 cylinder.

time for hydrate to cover the interface fully. Hydrate formation did not stop after a full coverage of the interface and the interfacial hydrate layer formed grew continuously which induced changes in rigidity and curvature of the interface. Hydrate growth apparently stopped when the interface became a planar surface because no further observable changes in hydrate-layer thickness were noticed. This hydrate growing process took about a few minutes. The thickness of the apparently stabilized hydrate layer was estimated to be in the range $80 \sim 100$ μm. Since hydrate was observed to form more easily near the surface of the sapphire tube, the tube surface may have a catalytic effect (this catalytic effect of a solid surface on hydrate formation has been noticed in many other systems); thus we believe that the hydrate-layer thickness may have been affected in some degree by the sapphire tube and a larger tube diameter may result in a thinner hydrate layer.

At $T > 10$°C, very similar interfacial phenomena to those below 10°C were observed. However, a significant difference is that the interface was often bumpy albeit its shapes were very similar to those observed at $T < 10$°C, which suggests that there may exist a difference in structure in some degree between the interfacial water above and below 10°C. To examine the difference in structure of the interfacial water at temperatures below and above 10°C, the interface was moved slowly via venting some liquid CO_2 out of the system while the pressure and temperature of the system remained constant. It was observed that at $T < 10$°C, when the interface moved upward the hydrate layer underwent cycles of collapse (into ice-like pieces) and reformation which was almost immediate. Collapse and reformation of the hydrate layer induced variations in shape and surface area of the interface: although the shape of the interface was often an oblique plane, the oblique angle varied from a few degrees to a very large value (sometimes even larger than 45°); however, there were no noticeable changes in the hydrate-layer thickness. At $T > 10$°C, the interfacial water behaved more like an assembly of many small solid pieces when the interface moved upward and the shape of the interface was an asymmetric convex surface rather than an oblique plane. In this case, since the interfacial water may resemble hydrate in local structure, i.e., at $T > 10$°C the interfacial water may have a quasi-crystalline structure. This argument is supported by the scanning electron microscopy of the supersaturated water reported by Ohgaki et al. [17].

2.3.2. *Behavior of the interface during CO_2 dissolution into water*

It has been mentioned in the introduction that crystallization (hydrate formation) at the interface does not stop mass transfer of CO_2 into water as long as the water is unsaturated with CO_2. The most interesting phenomena that we observed were variations in shape of the interface during the course of CO_2 dissolution into water. Since the pressure and temperature of the system

remained constant in each test, mass transfer of CO_2 into water caused a decrease in volume of the liquid CO_2 column which induced the interface to move upward at a rate of order of 10^{-4} mm s^{-1}. Various shapes of the interface were observed. Selected shapes of the interface are presented in Fig. 2. It is seen from Fig. 2 that the shapes of the interface above 10°C were very similar to those below 10°C, which supports the argument that at $T > 10$°C the interfacial water has a quasi-crystalline structure. In both cases, the oblique plane and the asymmetric convex were the most common shapes. The convex shape may be caused by the force balance at the interface: because the volume of the liquid CO_2 column decreased continuously due to mass transfer, the pressure of the liquid CO_2 column was always a little lower than that of the water column; thus the effective interfacial-tension pressure must be toward the water column to balance the pressure difference at the interface. However, the rigidity of the interface was variable around the surface and changed with time, as was reflected by various types of surfaces.

Behavior of the interfacial hydrate layer is of particular interest. The variation in shape and surface area of the interface suggests that the hydrate crystal may experience cycles of collapse and reformation. Collapse of the hydrate layer may be due to a physicochemical mechanism for instability [18] because the hydrate framework is unstable without filling a large percentage of its cavities with CO_2 molecules, or may be caused by the unbalanced forces at the interface. However, both mechanisms have a common cause—diffusion of CO_2 through the interfacial hydrate layer. Since the interface was always covered with hydrate at $T < 10$°C, it is reasonable to assume that hydrate reformation from collapsed hydrates is much faster than the initial setup. Behavior of the interface indicates that the interfacial hydrate layer is stable only in a chemical kinetic sense.

2.3.3. Interfacial mass transfer

Following the traditional practice, we may describe the interfacial mass transfer by Fick's law as:

$$\dot{m} = -D_s(\partial C/\partial x)_s, \tag{1}$$

or, alternatively, by the overall mass-transfer coefficient K as

$$\dot{m} = K(C_0 - C_w), \tag{2}$$

where $\dot{m}$ is the rate for mass transfer of CO_2 through the interface (unit area), and D_s and $(\partial C/\partial x)_s$ are the diffusion coefficient of CO_2 and the CO_2 concentration gradient at the interface of the water side; $C_0 \equiv \rho_{CO_2}/M_{CO_2}$, ρ_{CO_2} and M_{CO_2} are the density and molar mass of CO_2, respectively, and C_w is the concentration of CO_2 in the bulk water. Behavior of the interface suggests that equation (2) may be more appropriate to describe the interfacial mass transfer than equation (1). Equation (2) may be rewritten as

$$-\mathrm{d}(C_0 l)/\mathrm{d}t = K(C_0 - C_w), \tag{3}$$

where l is the length of the liquid CO_2 column. Since C_0 is constant at given pressure and temperature and $C_w \ll C_0$, equation (3) becomes

$$|\mathrm{d}l/\mathrm{d}t| = K(C_0 - C_w)/C_0 \approx K, \tag{4}$$

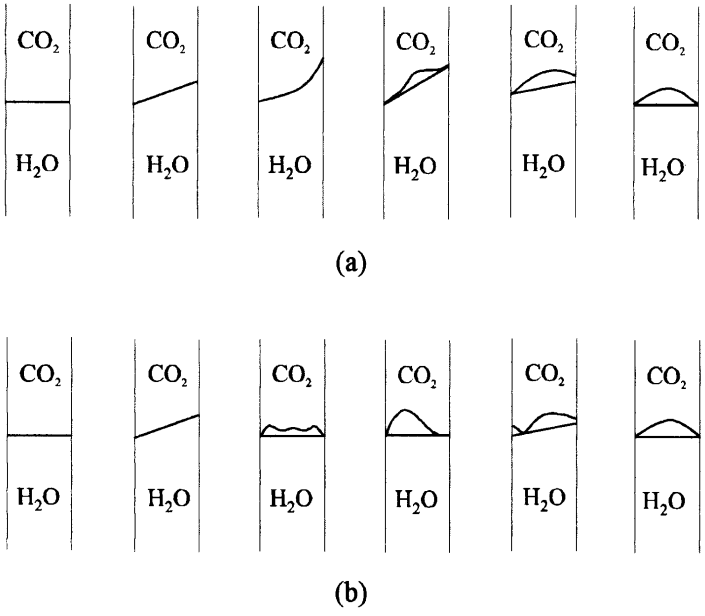

Fig. 2. Selected shapes of the liquid CO_2–water interface: (a) below 10°C; (b) above 10°C.

where $|dl/dt|$ is the shrinkage rate of the liquid CO_2 column. Thus $K \approx |dl/dt|$. Changes in l were recorded every hour during the course of CO_2 dissolution in each test and the rate of mass transfer was found to be basically independent of time. For each given temperature, tests were performed at six different pressures ($p = 60$, 100, 150, 200, 250, 300 bar); however, no obvious pressure dependence was noticed, as was found in dissolution of a CO_2 droplet in water [9, 13]. Therefore, the overall mass-transfer coefficient was obtained based on the averaged shrinkage rate for the six different pressures at each experimental temperature ($T = 5$, 8, 15, 18°C). The resultant overall mass-transfer coefficient K ($= 5.65 \sim 7.13 \times 10^{-7}$ m s^{-1}) as a function of temperature T is presented in Fig. 3.

It is seen from Fig. 3 that K increases with T and, evidently, hydrate formation does not induce a significant change in the rate of the interfacial mass transfer. Since diffusion coefficients both in solids and in liquids have an Arrhenius-type temperature dependence [16], the dependence of K on T may simply reflect this nature of diffusion in a condensed phase: increase in temperature enhances diffusion of CO_2 in both crystalline and quasi-crystalline interphases. The limited range of changes in K suggests that values of the activation energy for diffusion of CO_2 in crystalline and quasi-crystalline structure may not be different significantly. While the pressure independence of K may indicate that the variation with pressure of the local crystalline or quasi-crystalline structures may not be different significantly. While the pressure independence of K may indicate that the variation with pressure of the local crystalline or quasi-crystalline structure formed by hydrogen bonding of water molecules is very limited. As was noticed by Aya et al. [5–7] and Shindo et al. [13] in investigations of CO_2 dissolution in water, at a given temperature, the overall mass-transfer coefficient K is constant. This is due to the characteristics of the interfacial water and the CO_2–water system: As was mentioned in the preceding, hydrate forms only in the supersaturated interfacial layer where water has a quasi-crystalline local structure; thus hydrate formation does not change the local interfacial structure considerably [18]. When CO_2 dissolves in water, it reacts rapidly with water to form carbonic acid H_2CO_3, which subsequently yields bicarbonate ion HCO_3^- and carbonate ion CO_3^{2-}. Since carbonic acid is denser than water, it induces a downward transport (this downward convection was confirmed by using a pH indicator in our experiments). Because of these characteristics and the low solubility of liquid CO_2 in water, the overall resistance to and the driving force for the mass transfer varied only limited during the CO_2 dissolution, resulting in a constant overall mass-transfer coefficient. However, it needs to be pointed out that this constant mass-transfer rate holds only when the water-rich phase is highly unsaturated with CO_2.

Since the interfacial hydrate layer is very thin, the curvature of the interface may not affect the overall mass-transfer coefficient significantly. Therefore, the overall mass-transfer coefficient of the present study and that for a CO_2 droplet in water should be of the same order of magnitude if the diameter of the droplet is not very small. The corresponding form of equation (3) for a CO_2 droplet in water is

$$-\frac{d}{dt}\left(\frac{4}{3}r^3 C_0\right) = 4\pi r^2 K_d (C_0 - C_w), \tag{5}$$

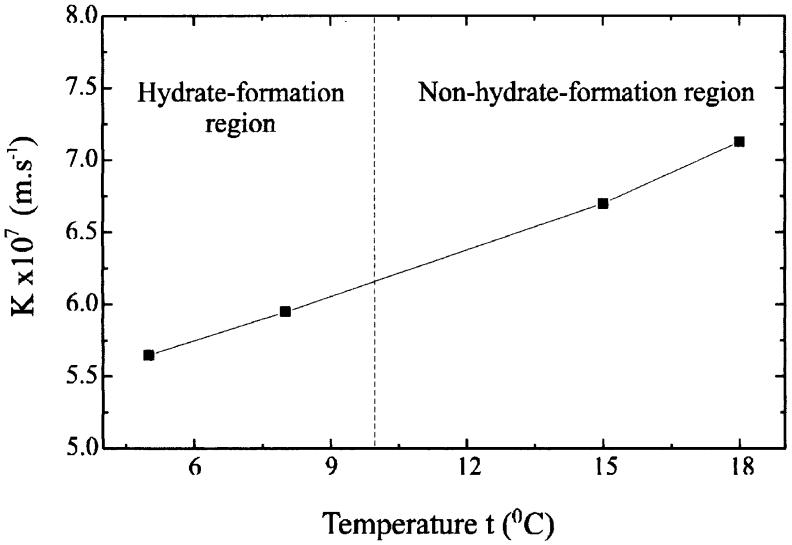

Fig. 3. Dependence of the overall mass-transfer coefficient on temperature.

where r is the droplet radius and K_d is the overall mass-transfer coefficient for the droplet. At given pressure and temperature, C_0 is constant; thus equation (5) may be rewritten as

$$|dr/dt| = K_d(C_0 - C_w)/C_0 \approx K_d, \quad (6)$$

where $|dr/dt|$ is the droplet-shrinkage rate. The droplet-shrinkage rate was measured previously by Aya et al. [5–7] and Fujioka et al. [9]. Within the hydrate-formation region, the values of $|dr/dt|$ obtained by Aya et al. is 4.67×10^{-7} m s^{-1} for $T = 1.9 \sim 7.2$°C [7] and by Fujioka et al. [9] is 2.5×10^{-7} m s^{-1} at $T = 3$°C. In the non-hydrate formation region, droplet-shrinkage rates were investigated only by Aya et al. Although in their early investigation Aya et al. [5] reported that $|dr/dt|$ was much larger than that in the hydrate-formation region, their most recent experiments showed that $|dr/dt| = 4.25 \sim 8.39 \times 10^{-7}$ m s^{-1} for $T \leqslant 15$°C [6, 7]. Evidently, the values for K obtained in the present study agree reasonably well with those for K_d obtained in previous investigations. However, the interfacial behavior was not revealed in previous investigations on dissolution of a CO_2 droplet in water, nor was the hydrate layer thickness.

3. Discussion

Behavior of the liquid CO_2–water interface during the course of CO_2 dissolution indicates that mechanism for mass transfer at the liquid CO_2–water interface may differ from that for the usual-type mass transfer that occurs in many other liquid–liquid systems. Since pressures and temperatures of deep-ocean waters fall within the hydrate formation region (note that conditions for hydrate formation are generally satisfied below 500 m in the ocean), the liquid CO_2–water interface (for hydration only water is relevant) covered with hydrate is of our interest. Hydrate formation at the interface and mechanism for the interfacial mass transfer will be discussed in this section.

3.1. Formation of hydrate at liquid CO_2–water interface

In this subsection, we discuss the initial setup of the hydrate layer at the interface. Hydrate formation is a kinetic process which may be expressed as

$$CO_2 + nH_2O \Rightarrow CO_2 \cdot nH_2O, \quad (7)$$

where n is the hydrate number. Based on the measured density of CO_2 hydrate, $n = 7.67$ [18], i.e., CO_2 hydrate is a non-stoichiometric compound. It may be assumed that the interfacial water is supersaturated with CO_2 initially and hydrate clusters form in water via diffusion of CO_2 in water. Hydrate formation is a complicated process involving several intermediate reactions for cavity formation and cavity association. The overall reaction for hydrate formation may be modeled as a first-order reaction on the basis of an apparent CO_2 concentration C_{app} as

$$\partial C_h/\partial t = \kappa C_{app}, \quad (8)$$

where C_h is the concentration of hydrate clusters in water and κ is the reaction-rate constant. C_{app} is related to the actual CO_2 concentration in water C as follows:

$$C_{app} = (1 - C_h/C_H)C, \quad (9)$$

where $C_H \equiv 5.76$ kmol m^{-3} is the hydrate density [18]. At the interface, equation (9) becomes

$$C_{app} = (1 - H)C_s, \quad (10)$$

where $H \equiv C_h/C_H$ and C_s is the CO_2 concentration at the interface. Combining equations (8) and (10) leads to

$$\partial H(t,x=0)/\partial t = \gamma(1 - H(t,x=0)), \quad (11)$$

where x denotes a distance from the interface and $\gamma \equiv \kappa C_s/C_H$. The solution to equation (11) is

$$H(t,x=0) = 1 - e^{-\gamma t}. \quad (12)$$

If we define the hydrate-formation time t_f by $H(t_f, x=0) \equiv 0.999$, then the reaction-rate constant may be derived from equation (12) as

$$\kappa = 6.91 C_H/(t_f C_s). \quad (13)$$

Based on our experiments, it may be estimated that $t_f \approx 13$ s and $C_s \approx 5.0$ kmol m^{-3} (here the coefficient of supersaturation is taken as 2.5 [19]). Substituting the values for C_H, t_f and C_s into equation (13) yields $\kappa = 0.61$ s^{-1}. Note that the value of κ may be system dependent because the primary nucleation period, the rate-controlling period in the hydrate-formation process, is noticed to vary with system [20].

Formation of the interfacial hydrate layer may be modeled by the following diffusion-reaction equation:

$$\frac{\partial C_{app}}{\partial t} = D\frac{\partial^2 C_{app}}{\partial x^2} - \kappa C_{app}, \quad t > 0, \quad 0 < x < \infty, \quad (14)$$

where D is the diffusion coefficient of CO_2 in water. The corresponding initial and boundary conditions for equation (14) are

$$C_{app}(0,x) = 0, \quad 0 \leqslant x < \infty, \quad (15)$$

$$C_{app}(t,0) = C_s e^{-\gamma t}, \quad (16)$$

$$C_{app}(t,\infty) = 0. \quad (17)$$

Here, the $x = 0$ boundary is modeled as a reaction boundary because hydrate formation at the interface is very rapid. A solution to equations (14)–(17) is obtained, employing Laplace transform, as

$$C_{app}(t,x) = \frac{C_s}{2} e^{-\gamma t}\left[e^{-\sqrt{\beta/D}x}\,\mathrm{erfc}\left(\frac{x}{\sqrt{4Dt}} - \sqrt{\beta t}\right) + e^{\sqrt{\beta/D}x}\,\mathrm{erfc}\left(\frac{x}{\sqrt{4Dt}} + \sqrt{\beta t}\right)\right], \quad (18)$$

where $\beta \equiv \kappa - \gamma$ and erfc represents the complementary error function. From equation (8),

$$\frac{\partial H(t,x)}{\partial t} = \frac{\gamma}{2} e^{-\gamma t}\left[e^{-\sqrt{\beta/D}x} \operatorname{erfc}\left(\frac{x}{\sqrt{4Dt}} - \sqrt{\beta t}\right) + e^{\sqrt{\beta/D}x} \operatorname{erfc}\left(\frac{x}{\sqrt{4Dt}} + \sqrt{\beta t}\right)\right]. \quad (19)$$

Integration of equation (19) between 0 and t yields

$$H(t,x) = \frac{\gamma}{2}\left[e^{-\sqrt{\beta/D}x} \int_0^t e^{-\gamma t'} \operatorname{erfc}\left(\frac{x}{\sqrt{4Dt'}} - \sqrt{\beta t'}\right) dt' + e^{\sqrt{\beta/D}x} \int_0^t e^{-\gamma t'} \operatorname{erfc}\left(\frac{x}{\sqrt{4Dt'}} + \sqrt{\beta t'}\right) dt'\right]. \quad (20)$$

The thickness of the hydrate layer δ should be evaluated after the hydrate concentration profile has developed fully (the corresponding time required may be assumed to be t^* and $t^* \gg t_f$ based on the experimental observations). Under such a condition, the hydrate concentration profile is, approximately,

$$H(x) \approx \exp(-\sqrt{\kappa/D}x). \quad (21)$$

If we define that $H(\delta) = 0.001$, then the thickness of the hydrate layer is

$$\delta = -\ln H(\delta)\sqrt{D/\kappa}. \quad (22)$$

The diffusion coefficient in the bulk water is $D \approx 2.0 \times 10^{-9}$ m^2 s^{-1} [21]. Because changes in structure of the interfacial water induce the diffusion coefficient to decrease significantly, it is reasonable to assume that $D \approx 10^{-10}$ m^2 s^{-1} in the interfacial water. Substituting the values for H, D, and κ into equation (22) yields $\delta = 88.5 \times 10^{-6}$ m (i.e., 88.5 μm), indicating that the hydrate layer is very thin. This prediction agrees with the experimental observation reasonably well.

3.2. Mechanism for mass transfer through interfacial hydrate layer

Mass transfer of CO_2 through the interfacial hydrate layer was proposed previously to follow an intermittent decomposition mechanism [10] which presumes that water diffuses into liquid CO_2 and reacts with CO_2 to form an impermeable hydrate layer; the hydrate layer decomposes in water and thus it is renewed following this same process. Alternatively, there may be a continuous decomposition mechanism [13, 22] which presumes that the hydrate layer is permeable to water (or to both water and CO_2) and that hydrate forms at the CO_2-rich interface and decomposes at the water-rich interface continuously. Both mechanisms assume that hydrate forms in the CO_2 phase. However, this assumption may be challenged on the basis that the mole fraction of water in hydrate is larger than 85% (which corresponds to the stoichiometric mole fraction) while the solubility of water in liquid CO_2 is less than 0.1% (which is less than that required for hydrate formation by more than two orders of magnitude) and, therefore, it is difficult for hydrate to form in the CO_2-rich phase, as was observed in our experiments. Thus the mechanism for the interfacial mass transfer should differ from those proposed previously. Based on the characteristics of hydrate, a plausible mechanism is proposed for mass transfer of CO_2 through the interfacial hydrate layer.

CO_2 and water are associated only via molecular forces in hydrate and the CO_2 molecule is smaller than the free diameter of most water cavities in hydrate; thus CO_2 can penetrate through hydrate. Although the water molecule (diameter 2.7 Å) is smaller than the CO_2 molecule, water molecules in liquid water exist in clusters with an average of 4.4 water molecules hydrogen bonded, indicating that it is difficult for water molecules to enter hydrate. Furthermore, since the broken hydrogen bonds of water molecules at the hydrate surface are arranged toward the water phase and interaction between water molecules at and in the vicinity of the hydrate surface is subject to an electrostatic force (note that each water molecule has four charges) which is much greater than the van der Waals driving force for water molecules to enter hydrate, water molecules are easily hydrogen-bonded at the hydrate face. This is consistent with the preceding argument that only CO_2 molecules can penetrate through the interfacial hydrate layer. The water (or mutual) diffusion concept [10, 13, 22] is contradictory to the fact that each water cavity in hydrate can hold at most one guest molecule and all of the cavities are occupied by CO_2 molecules at the stoichiometric condition. Even if water molecules enter the hydrate lattice, based on the guest-to-cavity size ratio rule for hydrate stability [23], they are too small to stabilize the cavities; otherwise water would form hydrate by itself. Because the framework of hydrate is formed with geometric distortions, the hydrate lattice by itself is unstable and its stability depends strongly on CO_2 occupancy [24].

The diffusive nature of CO_2 in hydrate indicates that establishment of the interfacial hydrate layer will not stop mass transfer from liquid CO_2 into water, which implies that if conditions for hydrate formation can be satisfied at the hydrate surface, the growth of the hydrate layer may continue. However, since molecular diffusion in solids is much slower than that in liquids, growth of the hydrate layer is much slower than the initial setup. This separates the initial setup and growth of the hydrate layer into two distinct states: the former is controlled by hydrate kinetics and the latter is governed by the rate of CO_2 transport. The mole fraction of CO_2 in hydrate $y^H_{CO_2}$ is regulated by the rates of mass transfer from liquid CO_2 into hydrate and from hydrate into water. The resistance to the CO_2 transport increases as the hydrate layer grows; thus, the rate of CO_2 transport from liquid CO_2 to the hydrate face decreases as the thickness of the hydrate layer increases. In comparison, the rate of CO_2

transport from hydrate into water changes only very limited as long as water remains highly unsaturated with CO_2. Once the rate of CO_2 transport from liquid CO_2 to the hydrate face is lower than that from hydrate into water, the number of CO_2 molecules leaving hydrate becomes larger than that of entering, causing $y^H_{CO_2}$ to decrease. Thus the hydrate layer grows with decrease in $y^H_{CO_2}$ and this will eventually cause the hydrate layer to become unstable. Once the hydrate layer collapses, the rate of CO_2 transport from liquid CO_2 into water increases significantly which results in reformation of hydrate at the interface. Since hydrate formation from collapsed hydrates is much faster than in the CO_2 supersaturated water, re-establishment of the hydrate layer is very rapid. During the course of CO_2 dissolution, the hydrate layer undergoes a continuous cycle of collapse and re-establishment, which results in variation in shape of the interface. Although the hydrate layer is thermodynamically unstable, rapid hydrate formation can maintain a hydrate layer at the interface during CO_2 dissolution and hence the hydrate layer may be considered to be chemical kinetically stable.

Based on our observations, the thickness of the hydrate layer is apparently unchanged during CO_2 dissolution. This may be explained as follows. The rates of transport of CO_2 from liquid CO_2 to the hydrate face and from hydrate into water may be expressed, respectively, as

$$\dot{m}_1 = D_H(C_0 - C_s)/\delta, \tag{23}$$

$$\dot{m}_2 = K_f(f^H_{CO_2} - f^W_{CO_2}), \tag{24}$$

where D_H is the interstitial-diffusion coefficient of CO_2 in hydrate, K_f is the mass-transfer coefficient based on fugacity, $f_{CO_2} = \gamma_{CO_2} y_{CO_2} f^0_{CO_2}$ is the fugacity, γ_{CO_2} is the activity coefficient, y_{CO_2} is the mole fraction of CO_2, $f^0_{CO_2}$ is the fugacity of pure liquid CO_2 at the same state, and the superscripts H and W denote the properties of hydrate and water phases, respectively. Since $y^H_{CO_2} \gg y^W_{CO_2}$, $f^H_{CO_2} \gg f^W_{CO_2}$. For a freshly-formed hydrate layer, it is reasonable to assume that

$$D_H(C_0 - C_s)/\delta \approx K_f \gamma^H_{CO_2} y^H_{CO_2} f^0_{CO_2}, \tag{25}$$

where $y^H_{CO_2} = 0.115$ (based on $n = 7.67$). Under the condition of equation (25), growth of the hydrate layer continues. Further growth of the hydrate layer leads to $\dot{m}_1 < \dot{m}_2$ which caused $y^H_{CO_2}$ to decrease. Decrease in $y^H_{CO_2}$, in turn, causes decrease in $f^H_{CO_2}$ and, therefore, reduces $\dot{m}_2$. Thus a new balance ($\dot{m}_1 = \dot{m}_2$) may be obtained. Through such regulations, the hydrate layer grow continuously with reducing the mole fraction of CO_2 in hydrate. After a certain number of cycles, the critical condition may be reached:

$$D_H(C_0 - C_s)/\delta_{cr} = K_f \gamma^H_{CO_2} y^H_{CO_2,cr} f^0_{CO_2}, \tag{26}$$

where the subscript cr denotes the properties at the critical condition (i.e., the minimum hydrate stability) and $y^H_{CO_2,cr} = 0.098$ [18]. Hydrate is a solid solution; thus, K_f and $\gamma^H_{CO_2}$ depend on $y^H_{CO_2}$ only slightly and may be treated as constant at given thermodynamic conditions. Then the ratio of δ_{cr} to δ may be derived from equations (25) and (26) as

$$\delta_{cr}/\delta = y^H_{CO_2}/y^H_{CO_2,cr} = 1.18. \tag{27}$$

Since $\delta_{cr} \sim \delta$ and collapse and re-establishment of the hydrate layer are all very rapid, the thickness of the interfacial hydrate layer appears unchanged during CO_2 dissolution. This gives an explanation to the apparently unchanged thickness of the hydrate layer.

Collapse of the hydrate layer may also have a mechanical mechanism, i.e., caused by unbalanced forces at the interface because mass transfer induces the interface to move toward the CO_2 phase. However, a sole mechanical mechanism cannot explain the kinetic behavior and the apparently unchanged thickness of the hydrate layer. Owing to the diffusive nature of CO_2 in hydrate (which also is the cause for the move of the interface), the CO_2 mole fraction in hydrate is variable and, accordingly, stability of hydrate will be influenced significantly by changes in the CO_2 mole fraction. Thus the physicochemical mechanism discussed above should be the major cause for the collapse; however, the shape of the interface is due to a certain type of force balance at the interface.

4. Summary and conclusions

Mass transfer through the liquid CO_2–water interface was investigated experimentally. Under high pressures and low temperatures, the solubility of water in liquid CO_2 is negligible in comparison with that of liquid CO_2 in water. Owing to this one-sided solubility feature and the characteristics of water, mass transfer at the liquid CO_2–water interface occurs in one way: only CO_2 can penetrate through the interface. Because of supersaturation with CO_2 and hydrogen bonding of water molecules, the interfacial water has a quasi-crystalline structure. If the pressure and temperature of the system fall within the hydrate-formation region, then hydrate will form rapidly at the interface; in this case, the quasi-crystal becomes a true crystal. The major experimental findings are summarized as follows:

(1) Hydrate formation at the interface was very rapid and it took less than 15 s for hydrate to cover the interface. The thickness of the interfacial hydrate layer was in the range 80 $\sim$ 100 μm which is close to that of the supersaturated interfacial water.
(2) Formation of the hydrate layer did not stop dissolution of CO_2 into water, however, mechanism for the interfacial mass transfer might differ from that for the usual-type mass transfer at a liquid–liquid

interface because the hydrate layer had kinetic behavior.

(3) Because the local structure of the interfacial water is similar to that of hydrate crystal, the interfacial crystallization did not change the rate of the interfacial mass transfer dramatically. The overall mass-transfer coefficients for the cases with and without an interfacial hydrate layer were of order of 10^{-7} m s^{-1}

(4) The overall mass-transfer coefficient depended only on temperature and increased with increasing temperature, which may reflect an Arrhenius-type temperature dependence of diffusion coefficients in hydrate and in water.

Kinetic behavior of the interfacial hydrate layer was discussed. The hydrate layer was assumed to undergo a continuous cycle of collapse and re-establishment during CO_2 dissolution into water. Based on the characteristics of hydrate, collapse of the hydrate layer was proposed to have a physicochemical mechanism, i.e., the CO_2 mole fraction in the hydrate layer becomes so small that it cannot satisfy the requirement by the minimum hydrate stability. This mechanism gives a reasonable explanation to the kinetic behavior of the hydrate layer and to the limited changes of the hydrate-layer thickness. The reaction-rate constant for hydrate formation was predicted from a first-order reaction model for hydrate formation and the measured hydrate-formation time. The hydrate-layer thickness was estimated based on a diffusion-reaction model and the hydrate-layer thickness predicted agreed reasonably well with that observed in experiments. The results of this study may be used as a basis for modeling dissolution of anthropogenic CO_2 disposed of in the deep ocean.

References

[1] T. Hakuta, Y. Shindo, Ocean and subterranean CO_2 disposal, Proceedings of the International Symposium on CO_2 Fixation and Efficient Utilization of Energy. Tokyo Institute of Technology, Tokyo, 1993, pp. 269–276.

[2] N. Nakashiki, T. Ohsumi, N. Katano, Technical view on CO_2 transportation onto the deep ocean floor and dispersion at intermediate depths, in: N. Handa, T. Ohsumi (Eds.), Direct Ocean Disposal of Carbon Dioxide, Terra Scientific Publishing Company, Tokyo, 1995, pp. 183–193.

[3] Y. Shindo, Y. Fujioka, M. Ozaki, K. Takeuchi, H. Komiyama, New concept of deep sea CO_2 sequestration, Proceedings of the International Symposium on CO_2 Fixation and Efficient Utilization of Energy, Tokyo Institute of Technology, Tokyo, 1993, pp. 307–314.

[4] T.R.S. Wilson, The deep ocean disposal of carbon dioxide, Energy Conversion and Management 33 (1992) 627–633.

[5] I. Aya, K. Yamane, N. Yamada, Feasibility study on the dumping of carbon dioxide in deep ocean, Proceedings of the First International Offshore and Polar Engineering Conference, Vol. 1, International Society of Offshore and Polar Engineers, Edinburgh, 1991, pp. 427–432.

[6] I. Aya, K. Yamane, N. Yamada, Stability of clathrate-hydrate of carbon dioxide in highly pressured water, in: P. G. Kroeger, Y. Bayazitoglu (Eds.), Fundamentals of phase change: freezing, melting and sublimation, ASME, 1992, pp. 17–22.

[7] I. Aya, K. Yamane, N. Yamada, Effect of CO_2 concentration in water on the dissolution rate of its clathrate, Proceedings of the International Symposium on CO_2 Fixation and Efficient Utilization of Energy. Tokyo Institute of Technology, Tokyo, 1993, pp. 351–360.

[8] I. Aya, K. Yamane, N. Yamada, Simulation experiment of CO_2 storage in the basin of deep ocean, Energy Conversion and Management 36 (1995) 485–488.

[9] Y. Fujioka, K. Takeuchi, Y. Shindo, H. Komiyama, Shrinkage of liquid CO_2 droplet in water, International Journal of Energy Research 18 (1994) 765–769.

[10] P.C. Lund, Y. Shindo, Y. Fujioka, H. Komiyama, Study of the pseudo-steady-state kinetics of CO_2 hydrate formation and stability. International Journal of Chemical Kinetics 26 (1994) 289–297.

[11] P.C. Lund, The effect of CO_2-hydrates on deep ocean carbon dioxide deposition options, Energy Conversion and Management 36 (1995) 543–546.

[12] T. Ohsumi, N. Nakashiki, K. Shitashima, K. Hirama, Density change of water due to dissolution of carbon dioxide and near-field behavior of CO_2 from a source on deep-sea floor. Energy Conversion and Management 33 (1992) 685–690.

[13] Y. Shindo, Y. Fujioka, K. Takeuchi, H. Komiyama, Kinetics on the dissolution of CO_2 into water from the surface of CO_2 hydrate at high pressure, International Journal of Chemical Kinetics 27 (1995) 569–575.

[14] S.M. Walas, Phase Equilibria in Chemical Engineering, Butterworth, Boston, 1985.

[15] H. Teng, C.M. Kinoshita, S.M. Masutahi, Hydrate formation on the surface of a CO_2 droplet in high-pressure, low-temperature water, Chemical Engineering Science 50 (1995) 559–564.

[16] W. Jost, Diffusion in Solids, Liquids, and Gases, Academic Press, New York, 1952.

[17] K. Ohgaki, N. Kirokawa, M. Ueda. Heterogeneity in aqueous solutions: electron microscopy of citric acid solutions, Chemical Engineering Science 47 (1992) 1819–1823.

[18] H. Teng, A. Yamasaki, Y. Shindo, Stability of the hydrate layer formed on the surface of a CO_2 droplet in high-pressure, low-temperature water, Chemical Engineering Science 51 (1996) 4979–4986.

[19] H. Teng, A. Yamasaki, Dissolution of CO_2 droplets in the ocean, Energy—The International Journal 22 (1997) 751–761.

[20] E.D. Sloan Jr, Conference Overview, in: E.D. Sloan Jr, et al. (Eds.), International Conference on Natural Gas, The New York Academy of Science, New York, 1994, pp. 1–23.

[21] D. Golomb, H. Herzog, J. Tester, D. White, S. Zemba, Feasibility, modeling and economics of sequestering power plant CO_2 emissions in the deep ocean, Energy Laboratory Report, MIT-EL 89-003, MIT, Cambridge, 1989.

[22] Y. Mori, T. Mochizuki, Modeling of mass transfer across a

hydrate layer intervening between liquid water and "guest" fluid phases, Proceedings of the Second International Conference on Natural Gas Hydrates, Toulouse, France, 1996, pp. 267–274.

[23] E.D. Sloan Jr, F. Fleyfel, A molecular mechanism for gas hydrate nucleation from ice, AIChE Journal 37, (1991) 1281–1292.

[24] H. Teng, Comment: Characteristics of the hydrate layer formed at the liquid CO_2–water interface, International Journal of Chemical Kinetics 28 (1996) 935–937.